DØ Note 2632

Rapidity Gaps between jets at DØ and CDF

Iain Bertram[1]

Rice University, Houston, Texas 77251

Results are presented from analyses of particle multiplicity distributions between high transverse energy jets produced at the Fermilab Tevatron $p\overline{p}$ collider at $\sqrt{s} = 1.8$ Tev. DØ and CDF examine the particle multiplicity distribution between the two highest transverse energy jets. Both experiments observe a significant excess of events at low tagged particle multiplicity which is consistent with a strongly interacting color–singlet exchange process.

INTRODUCTION

Rapidity gaps, namely regions of rapidity containing no final–state particles, are expected to occur between jets when a color–singlet is exchanged between the interacting hard partons (1). The exchange of a photon (2), W boson, Z boson or a hard QCD Pomeron (3,4) is expected to give such an event topology. Although the cross section for electroweak gauge boson exchange is small, the cross section for two–gluon Pomeron exchange is believed to be significant (3,5), and roughly 10% of jet events may be due to Pomeron exchange (3). Typical color–exchange jet events (single gluon or

[1]To be published in the Proceedings of the 10th Topical Workshop on Proton Antiproton Collider Physics, May 9 – 13, 1995, Fermilab, Batavia, Illinois.

quark exchange) have particles between jets, but rapidity gaps can arise from fluctuations in the particle multiplicity, which is expected to have a negative binomial or similar distribution (6). These "background" rapidity gap events are expected to become highly suppressed as the jet rapidity separation is increased.

Rapidity gaps will not be observed in the final state, however, if spectator interactions produce particles between the jets. Approximately 10–30% of rapidity gap events are expected to survive spectator interactions (3,7). Thus roughly 1–3% of jet events are expected to have an observable rapidity gap between the jets from Pomeron exchange.

Although it is not possible to distinguish color–singlet rapidity gaps from those that occur in color–octet exchange on an event–by–event basis, differences in the expected particle multiplicity distributions can be used to search for a color–singlet signal. This signal is expected to appear as an excess of events at low particle multiplicity compared to a negative–binomial–like distribution.

Experimentally, both DØ and CDF measure the multiplicity of particles in the pseudorapidity interval ($\Delta\eta_c = |\eta_1 - \eta_2| - 2\mathcal{R}$) between the cone edges ($\mathcal{R} = \sqrt{\Delta\eta^2 + \Delta\phi^2} = 0.7$) of the two highest E_T jets (Fig 1).

The DØ collaboration has published a study of rapidity gaps between jets (8). Although rapidity gaps were observed with an experimental definition (no electromagnetic towers of $\Delta\eta \times \Delta\phi = 0.1 \times 0.1$ with more than 200 MeV), this did not directly imply color singlet exchange because inefficiencies could have created false gaps, and there was an indeterminate background from

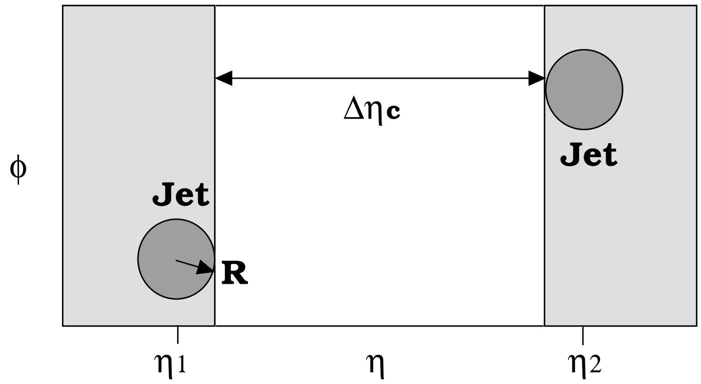

FIG. 1. Representation in η–ϕ space of the distribution of particles in a typical two–jet event containing a rapidity gap. The pseudorapidity region between the edges of the jet cones (of radius $\mathcal{R}$), $\Delta\eta_c = |\eta_1 - \eta_2| - 2\mathcal{R}$, contains no particles.

particle multiplicity fluctuations in color–exchange events. An upper limit was placed on the fraction of events with a rapidity gap between the jets (1.1% at 95% CL) (8).

The CDF Collaboration has published (9) the fraction of jet events with a rapidity gap using charged tracks with $p_T > 400$ MeV. They also observed rapidity gaps, but used a smooth fit to the tracking multiplicity distribution to estimate the background from fluctuations. They quote a fraction of $0.0085 \pm 0.0012(stat)^{+0.0012}_{-0.0024}(sys)$.

This report will describe the status of the current DØ and CDF rapidity gap analyses.

CDF ANALYSIS

The data set used in the CDF analysis of rapidity gaps require that there be two jets in the forward calorimeters (the detector is described elsewhere (10)) with $E_T > 20$ GeV. After removing bad runs, there are 5634 events with zero or one interaction vertices. The effective luminosity of this sample is approximately 50 nb^{-1}. These events were then required to have an interaction vertex $<$ 60 cm from the detector center and two jets with $E_T > 20$ GeV and a detector pseudorapidity ($\eta_{\rm detector}$) greater than 1.8.

A set of additional cuts is made to ensure that the final data sample is free of background or mis–measured jets. The two leading jets were required to be back–to–back in ϕ and roughly balanced in E_T. The leading jet E_T was also required to be less than 60 GeV. These cuts preferentially remove color–exchange events with a large amount of radiation and thus bias the relative rate estimate slightly. A total of 4469 events (3415 events with jets on the same side (SS) of the calorimeter and 1054 with the jets on opposite sides (OS) of the calorimeter) pass these cuts.

The particle multiplicity distribution between jets is determined using tracks in the Central Tracking Chamber (CTC). A track is used if it has a transverse momentum (p_T) $>$ 300 MeV and the difference between intercept between the track and the event vertex satisfy the following conditions; $\mid z_{\rm track} - z_{\rm vertex} \mid < 8.0\, cm$ and $\{(x_{\rm track} - x_{\rm vertex})^2 + (y_{\rm track} - y_{\rm vertex})^2\}^{1/2} < 0.8\, cm$. The tracking efficiency for the CTC starts to fall steeply for $p_T < 300$ MeV and for $\eta > 1.2$.

The track multiplicity distributions for $\Delta\eta_d > 2.2$ (where $\Delta\eta_d$ is the overlap between $\Delta\eta_c$ and the CTC) OS and for $\Delta\eta_d > 2.4$ for SS events are shown in Fig 2(a). The number of SS events has been normalized to the number of OS events excluding the zero multiplicity bin. The mean multiplicity for OS events is approximately 10% higher than that of SS events. For this reason the SS rapidity region was chosen to be somewhat wider than that of the OS

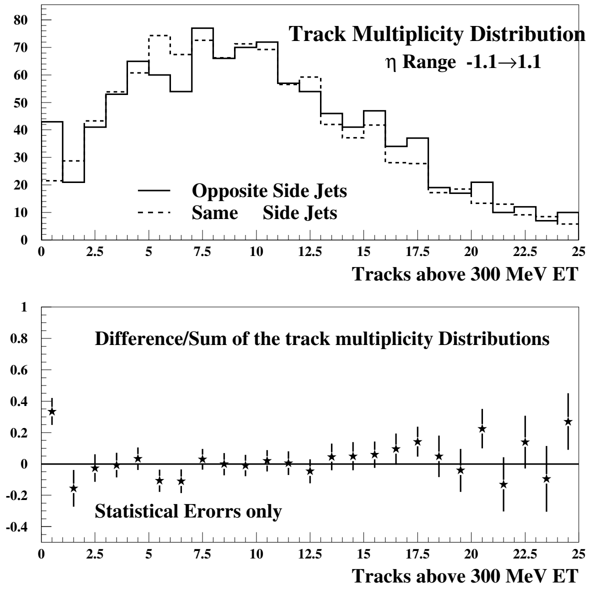

FIG. 2. (a) Track multiplicity distributions for OS ($|\eta| < 1.1$, mean=9.87 tracks) events and SS ($|\eta| < 1.2$, mean=9.73) events. The number of SS events has been normalized to the number of OS events excluding the zero–track bin. (b) The difference/sum of the OS and SS distributions.

events. For example, the OS multiplicity distribution in the region $|\eta| < 1.1$ is compared with the SS multiplicity distribution in the region $|\eta| < 1.2$.

Figure 2(b) shows the difference/sum of the normalized multiplicities. For each bin the ratio (r_i) and its error (e_i) are given by:

$$r_i = \frac{N^i_{\rm OS} - C N^i_{\rm SS}}{N^i_{\rm OS} + C N^i_{\rm SS}} \tag{1}$$

$$e_i = \frac{2C\sqrt{N^i_{\rm OS} N^i_{\rm SS} \left(N^i_{\rm OS} + N^i_{\rm SS}\right)}}{\left(N^i_{\rm OS} + C N^i_{\rm SS}\right)^2} \tag{2}$$

where $N^i_{\rm OS}$ and $N^i_{\rm SS}$ are the number of OS and SS events in the i–th bin and C is the overall normalization factor which is assumed to have no error. For $|\eta| < 1.1$ there is an excess of 21.5 ± 7.0 events in the zero multiplicity bin. The measurement is repeated for several different $|\eta|$ ranges and the results

TABLE 1. Number of events with no tracks for various η ranges

η Range	Same Side Jets Events		Opposite Side Jets Events		Results	
	$<$ Mult $>$	0–bin	$<$ Mult $>$	0–bin	Prediction from SS	Excess in 0–track bin
-0.9–0.9	8.14	101	8.04	48	30.7±3.1	17.3±7.6
-1.0–1.0	8.95	83	8.95	44	25.2±2.8	18.8±7.2
-1.1–1.1	9.73	71	9.87	43	21.5±2.5	21.5±7.0
-1.2–1.2	10.49	62	10.76	43	18.7±2.4	24.3±7.0
-1.3–1.3	11.16	55	11.54	41	16.8±2.2	24.4±6.8
-1.4–1.4	11.68	52	12.21	37	15.7±2.2	21.3±6.5
-1.5–1.5	12.07	48	12.71	32	14.6±2.1	17.4±6.0

are given in Table 1. The size of the excess of events in the zero multiplicity bin remains consistent within statistical errors.

To verify that the zero–track events are not caused by a detector effect, the correlations between track and calorimeter tower multiplicities were examined. The tower multiplicity is shown (for OS events in the region $|\eta| < 1.1$) in Fig. 3. An excess of events in the OS tower multiplicity distributions where the $n_{towers} = 0$ to 3 is observed which is consistent with the excess of events observed in the zero–track multiplicity bin. The tower multiplicity is on average higher than the track multiplicity because the calorimeter detects both neutral and charged particles, has a lower energy threshold, and also detects additional particles due to showering initiated outside of the gap region.

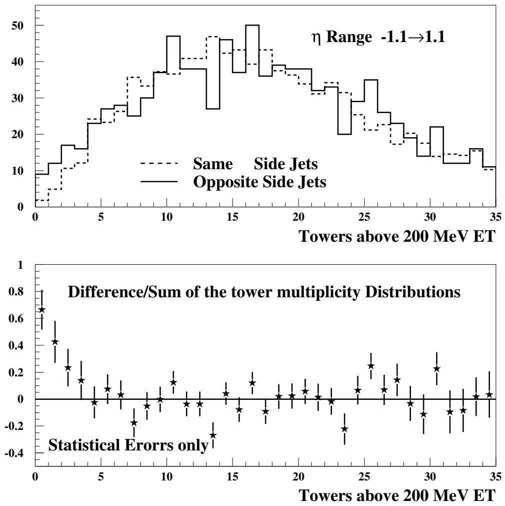

FIG. 3. (a) Tower multiplicity distributions for OS ($|\eta| < 1.1$, mean=18.49 tracks) events and SS ($|\eta| < 1.2$, mean=18.73) events. (b) The difference/sum of the OS and SS distributions.

DØ ANALYSIS

The data sample used in the DØ analysis is derived from a special high–$\Delta\eta_c$ trigger (8) implemented to obtain events with large pseudorapidity separation ($\Delta\eta_c$) between the cone edges of the two highest E_T jets (see Fig 1). In the offline analysis, events are required to have at least two jets, each with $E_T > 30\,\mathrm{GeV}$ and $|\eta| > 2$. Events with more than one interaction in a proton–antiproton crossing are removed since they include a source of particles not associated with the triggering interaction. The effective luminosity of this data sample is approximately 5.4 pb^{-1} (corresponding to approximately 15,000 events). The calorimeter (11) is used to measure the multiplicity distribution of tagged particles between the two highest E_T jets (where the number of tagged cells is given by N_{EM}). Particles are tagged in the electromagnetic section of the calorimeter by requiring $E_T > 200\,\mathrm{MeV}$ in a calorimeter tower (8).

Although the color–exchange particle multiplicity between jets is expected to have a negative binomial–like distribution, it is important to show that detector effects do not cause a significant deviation from the expected distribution, especially at low multiplicity. The Monte Carlo PYTHIA has been shown to be consistent with negative binomial particle multiplicity distribution between jets for events generated with conditions similar to the high–$\Delta\eta_c$ trigger (12). Propagation through a simulation of the DØ geometric acceptance and particle tagging efficiency gives a multiplicity distribution which is also consistent with a negative binomial distribution. No deviation is observed at low multiplicity, indicating that detector effects do not generate an artificial excess.

An enriched color–exchange subsample of the data was also studied. This sample was obtained by requiring a jet ($E_T >$8 GeV) to be in the $\Delta\eta_c$ region between the two leading jets. Figure 4(a) shows the tagged particle multiplicity distribution between the two highest E_T jets for $\Delta\eta_c > 3$. Another control sample of data consisted of events in which the two leading E_T jets were found on the same side of the detector. To remove any color–singlet contribution to this sample from hard single diffractive events from this sample a beam–beam coincidence was required (produced by the break up of the proton and anti–proton). Figure 4(b) shows the multiplicity in a region of $\Delta\eta = 2.4$ centered around $\eta = 0$ for these events. Both distributions are consistent with a negative binomial distribution which demonstrates that detector effects do

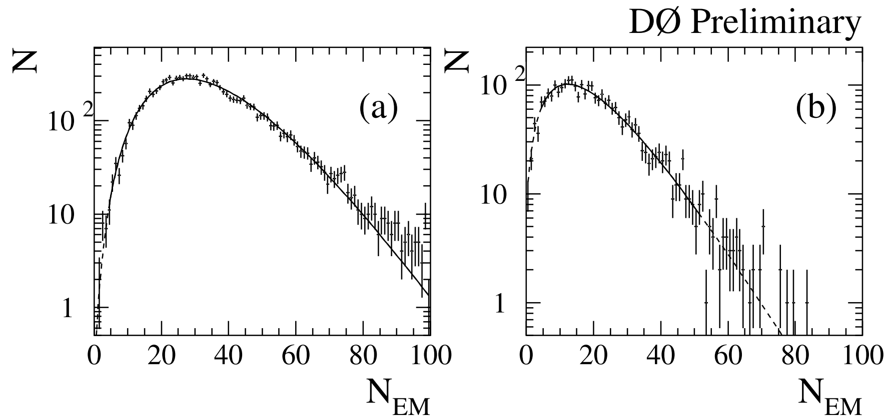

FIG. 4. The tagged particle multiplicity distributions obtained from color–octet events, for the data sample where a jet is required to be in the region $\Delta\eta_c$ (a) and for a sample of events where both jets are on the same side of $\Delta\eta_c$ (b). Negative binomial fits to the data (solid lines) are also shown.

not produce an excess of events at low multiplicities.

The inclusive tagged–particle multiplicity distribution for events with $\Delta\eta_c > 3$ is shown in Fig. 5, with the bottom figure showing the same quantity on a log–log scale. A significant excess is observed at small particle multiplicity ($N_{\rm EM} < 4$) compared to a negative binomial (dashed curve) and double negative binomial fit (solid curve). The preliminary excess is $263 \pm 21(stat) \pm 10(sys)$ events for the single negative binomial and $154 \pm 21(stat) \pm 16(sys)$ for the double negative binomial, where the systematic error currently only includes the error on the fit parameters. The starting bin of the fit of $N_{\rm EM} = 4$ has been chosen to minimize the resulting χ^2. Although both distributions give a $\chi^2 \approx 1$, shape tests show systematic differences between the single negative binomial and the data. The double negative binomial (sum of two negative binomials), which has a better shape agreement and a somewhat smaller excess, is thus introduced. Monte Carlo

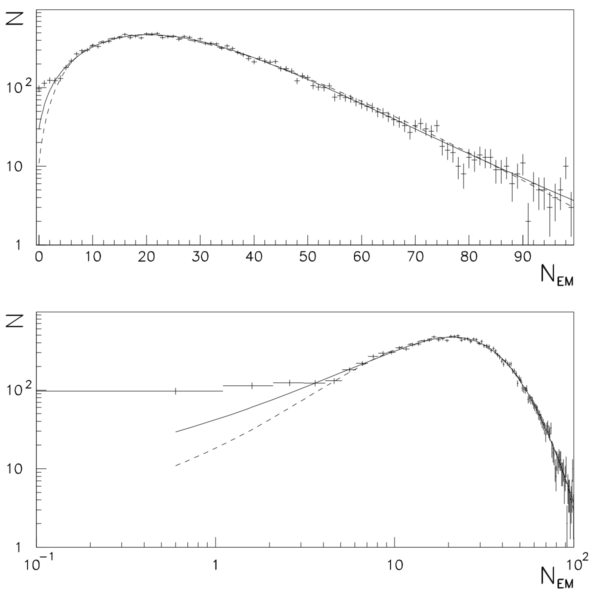

FIG. 5. The preliminary tagged–particle multiplicity distributions obtained from the inclusive event sample for $\Delta\eta_c > 3$. A negative binomial fit to the data for $N_{\rm EM} \geq 4$ and extrapolated to $N_{\rm EM} = 0$ is shown (dashed line) as well as a double negative binomial fit (solid line).

studies show that the double negative binomial may arise from the fact that two sub-processes qg and qq with different multiplicity distributions are the dominant contributors to the event topologies under study. It should be noted that the Monte Carlo and data background distributions give no excess for single or double negative binomial fits.

The excess above the fit has been determined by subtracting the fit from the data for $N_{\rm EM} < 4$. A preliminary fractional excess of

$$f = \frac{N(N_{\rm EM} < 4)}{N_{total}} = (0.9 — 1.5 \pm 0.1(stat)) \times 10^{-2}$$

is obtained where the upper edge of the range comes from the single negative binomial fit and the lower edge of the range is determined using the more

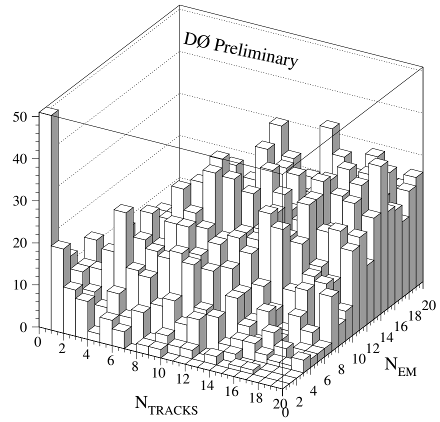

FIG. 6. The multiplicity of tracks in the CDC vs. the multiplicity of electromagnetic calorimeter towers ($n_{\rm EM}$).

conservative double negative binomial fit. The systematic error is currently under study, but it is clear that the largest component of the error is the fitting of the background shape.

To verify that the excess of data above the fit is not caused by a detector effect, the correlation between $N_{\rm EM}$ and the number of tracks observed in the Central Drift Chamber (CDC) (11) is examined for the region of η–ϕ space where the two detector systems overlap. It is clear from the lego plot shown in Fig. 6 that $N_{\rm EM}$ and the number of tracks seen in the CDC is highly correlated and that there is a significant excess of events in the zero–track/zero–tower bin.

DØ has previously published (8) the fraction of events which have zero electromagnetic towers ($N_{\rm EM} = 0$) as a function of $\Delta\eta_c$. This result has been compared to the value of the negative binomial fit for the $N_{\rm EM} = 0$ bin as shown in Fig. 7. While the fraction of events with $N_{\rm EM} = 0$ (solid circles) remains constant for $\Delta\eta_c > 2$, the value from the zero bin of the fit (open

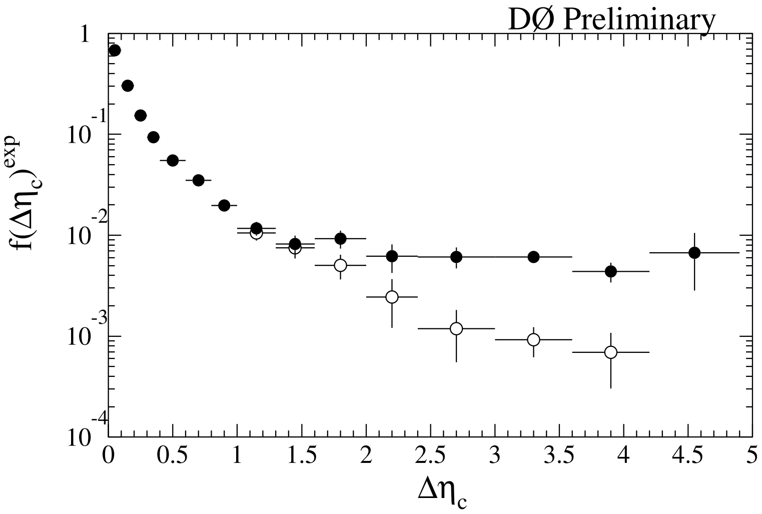

FIG. 7. The fraction of events that have no tagged particles between the two leading jets (solid circles) and the value of the negative binomial fit for the no tagged particle multiplicity bin (open circles) as a function of $\Delta\eta_c$. The error bars show the statistical uncertainty only

circles), which represents color–exchange, decreases rapidly. The difference between the two curves could be attributed to the portion of color–singlet exchange events which have no struck calorimeter towers between the jets. This also points out why the upper limit of 1.1% is not inconsistent with the excess of 0.9—1.5%, as the upper limit only includes rapidity gap events which survive spectator interactions, while the excess above the fit also could include those color–singlet events which have a low multiplicity spectator interaction.

CONCLUSION

Both CDF and DØ have measured the tagged particle distributions between jets. Both experiments observe a significant excess of events at low tagged multiplicity compared to an assumed background form for the color–

octet exchange background. The measured fractional excess for both experiments is:

$$\text{CDF}: \quad 2.0 \pm 0.7(\text{stat})\% \quad (\Delta\eta_c > 2.2, E_T > 20 \text{ GeV}) \tag{3}$$

$$\text{DØ}: \quad 0.9 — 1.5 \pm 0.1(\text{stat})\% \quad (\Delta\eta_c > 3, E_T > 30 \text{ GeV}) \tag{4}$$

The excess measured by both experiments is consistent to within the statistical errors. The measured excess for both CDF and DØ is approximately ten times larger than predicted excess due to electroweak exchange (13) ($\sigma/\sigma_{\text{EW}}$). However, a direct comparison with theory is difficult due to uncertainties in the assumed background shape and uncertainty of survival probability and spectator multiplicity.

The observed excess is consistent with expectations for a strongly interacting color–singlet exchange process, at a level considerably larger than expected for electroweak color–singlet exchange, thus suggesting the existence of a strongly interacting exchange mechanism.

We are grateful to the DØ and CDF Collaborations for discussions of their data. We appreciate the substantial contributions to this work on the part of the Fermilab Accelerator, Computing and Research Division staffs.

REFERENCES

1. Y. Dokshitzer, V. Khoze and S. Troyan, *Proc. of the 6th Int. Conf. on Phys. in Collisions* (1986), ed. M. Derrick (World Scientific, Singapore, 1987).
2. R. S. Fletcher and T. Stelzer, Phys. Rev. **D48**, 5162 (1993).
3. J. D. Bjorken, Phys. Rev. **D47**, 101 (1992).

4. H. Chehime and D. Zeppenfeld, preprint MAD/PH/814 (1994).
5. V. Del Duca and W. K. Tang, preprint SLAC-PUB-6310 (1993).
6. I. Dremin, submitted to Physics Uspekhi, FIAN **TD-6**, (1994) and references therein.
7. E. Gotsman, E. M. Levin and U. Maor, Phys. Lett. **B309**, 199 (1993).
8. S. Abachi *et al.* (DØ Collaboration), Phys. Rev. Lett. **72**, 2332 (1994).
9. F. Abe *et al.* (CDF Collaboration), Phys. Rev. Lett. **74**, 855 (1995).
10. F. Abe *et al.* (CDF Collaboration), Nucl. Inst. and Meth. **A271**, 387 (1988)
11. S. Abachi *et al.* (DØ Collaboration), Nucl. Inst. and Meth. **A338**, 185 (1994)
12. R. Fletcher, private communication.
13. H. Chehime *et al.*, Phys. Lett. **B286**, 397 (1992)